17th World Conference on Earthquake Engineering, 17WCEE
Sendai, Japan - September 13th to 18th 2020

Shear behavior of DFRCC coupling beams using PVA and aramid fibers

D. Sunaga[1], K. Namiki[2], T. Kanakubo[3]

[1],[2] *Graduate student, Graduate School of System and Information Engineering, University of Tsukuba, Ibaraki, Japan*
[1] *s1920914@s.tsukuba.ac.jp,* [2] *s1820921@s.tsukuba.ac.jp*
[3] *Professor, Department of Engineering Mechanics and Energy, University of Tsukuba, Ibaraki, Japan, kanakubo@kz.tsukuba.ac.jp*

Abstract

Ductile fiber-reinforced cementitious composite (DFRCC) is expected to provide sufficient shear performance of coupling beams in high-rise buildings under severe seismic loads and decrease the deterioration of energy absorption performance. This study focuses on shear behavior of coupling beams through anti-symmetrical loading test of beam specimens using PVA and aramid fiber-reinforced cementitious composite. The test parameters are fiber types, volume fraction of fibers and diameter of stirrup. According to the test results, most of the specimens with fibers showed higher value of shear capacity than mortar specimens. The shear capacity is evaluated by using tensile strength of DFRCC obtained by four-point bending test of test pieces. In most of the specimens, calculated shear capacities showed good agreements with the test results.

Keywords: Shear Behavior; DFRCC; Coupling Beams; PVA fiber; Aramid fiber

1. Introduction

Ductile Fiber-Reinforced Cementitious Composite (DFRCC), which shows a deflection hardening branch and multiple cracking under bending stress, have been focused by lots of researchers because of its unique mechanical performance. In other hand, Engineered Cementitious Composite (ECC), which has been introduced by Li [1], exhibit a maximum tensile strain of several percent owing to the synergetic effect of high-performance fiber under pure tension. Unprecedented high-performance structural members by ECC have already been applied to seismic components such as coupling beams [2].

Previous study has reported that structural members using DFRCC shows less damages and small crack opening compared with conventional concrete members [3]. DFRCC can also make it possible to improve durability and sustainable use of structures. However, it is difficult to evaluate tensile characteristic of DFRCC and structural performance of seismic components.

In the case of ECC, it is not so difficult to evaluate its tensile characteristic because of strain hardening behavior. Tensile stress increases after first cracking, and tensile stress carrying capacity does not start failing until cracks saturating. For example, bi-linear model with hardening branch or perfectly elastic-plastic model can be applied to express the tensile stress-tensile strain relationship for ECC [4]. In fact, Kanakubo et al. have proposed the evaluation method of tensile strength of ECC by four-point bending test results as the material test of ECC [5]. In the case of DFRCC, however, its tensile stress generally starts decreasing after peak load in pure tension stress field. So, it is difficult to confirm the carrying tensile stress by DFRCC on its softening branch in seismic components.

In previous study [6], to evaluate shear behavior of DFRCC coupling beams as seismic component, anti-symmetrical loading test of beam specimens using PVA and steel fiber-reinforced cementitious composite was conducted. In this study, to accumulate more data about DFRCC coupling beams, additional loading test of beam specimens using DFRCC was conducted by further test parameters. 2 types of PVA fibers and aramid fiber are used for DFRCC. In addition to that, diameter of stirrups is also changed as the test parameter to

discuss the interaction between fiber bridging effect and contribution of stirrups. The shear capacity is evaluated by using tensile strength of DFRCC obtained by four-point bending test of test pieces.

2. Outline of loading test for beam specimens

2.1 Specimen

Fig. 1 shows the dimensions of beam specimen and Table 1 shows the specimens list. The total length of the specimen is 1,960mm. The central portion of 660mm length is the test region which is subjected to the anti-symmetrical bending moment. The depth (D) and width (b) of cross-section is 220mm and 160mm, respectively. Table 2 lists the mechanical properties of steel rebars. Three steel deformed rebars D16 (SD490) were arranged as tension longitudinal reinforcements to avoid flexural yielding before shear failure.

The test parameters are diameter of stirrup, types of fiber for DFRCC and volume fraction of fiber. Steel deformed rebars D4 or D6 (SD295) were arranged as stirrups at 120mm interval in the test region. Table 3 shows the dimensions and mechanical properties of fibers. 2 types of PVA fiber with 100μm diameter and 27μm diameter, and aramid fiber with 12μm diameter were used for DFRCC. Fiber volume fraction was set to 1.0% and 2.0% for φ100 PVA fiber, 0.5% for φ27 PVA fiber and aramid fiber. NF-D4, PVA10-D4 and PVA20-D4 specimens are tested in previous study as No.1 ~ No.3 [6].

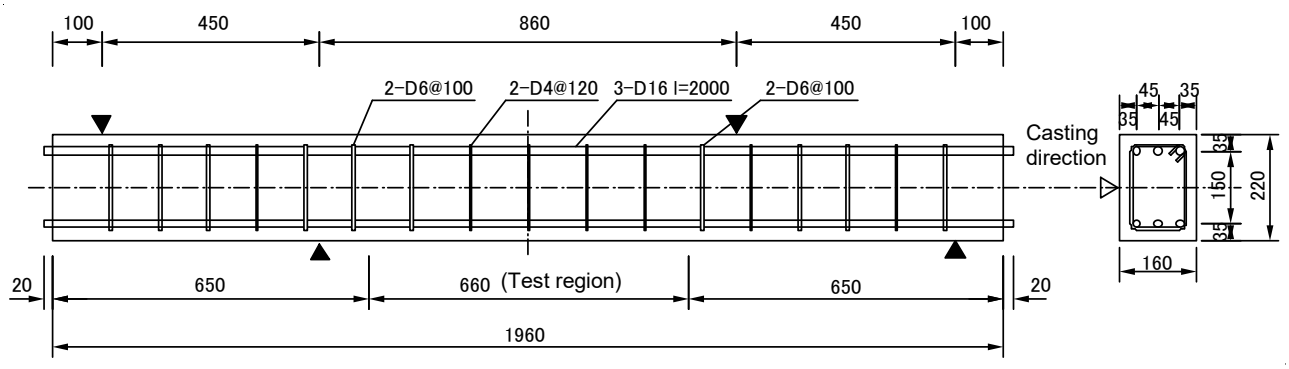

Fig. 1 Specimen dimensions

Table 1 Specimens list

ID	Common factor	Fiber		Stirrup Type (p_w)
		Type	Volume fraction	
NF-D4 (No.1[6])	Cross-section: 160x220mm Shear span: 330mm (M/QD=1.5) Tension bar: 3-D16 (SD490) Stirrup: D4 or D6@120 (SD295)	-	-	D4 (0.15%)
NF-D6				D6 (0.33%)
PVA10-D4 (No. 2 [6])		PVA (φ100μm)	1.0%	D4 (0.15%)
PVA10-D6				D6 (0.33%)
PVA20-D4 (No. 3 [6])			2.0%	D4 (0.15%)
PVA20-D6				D6 (0.33%)
PVA'05-D4		PVA (φ27μm)	0.5%	D4 (0.15%)
PVA'05-D6				D6 (0.33%)
AR05-D4		Aramid (φ12μm)	0.5%	D4 (0.15%)
AR05-D6				D6 (0.33%)

Table 2 Mechanical properties of steel rebar

Type	Diameter	Yield strength (MPa)	Elastic modulus (GPa)	Remarks
SD490	D16	520	195	Longitudinal bar
SD295	D4	380	183	Stirrup
	D6	393	204	

Table 3 Mechanical properties of fiber

Fiber type	Diameter (μm)	Length (mm)	Tensile strength (MPa)	Elastic modulus (GPa)
PVA	100	12	1200	28
	27	6	1800	45
Aramid	12	12	3410	41

PVA (φ100μ) PVA'(φ27μ) Aramid

Fig. 2 Visual appearance of fibers

2.2 Loading and measurement

The monotonic loading following anti-symmetric bending moment manner (Ohno-type shear test method) was conducted. The bending moment diagram is shown in Fig. 3. Applied shear force (Q) can be obtained by 0.344 times applied force (P).

To avoid shear failure outside the test region, both ends of beam specimen were jacketed by steel plates with 22 mm thickness as shown in Fig. 4. Steel round bars were placed at both loading points and supports. Fig. 5 shows the state of loading.

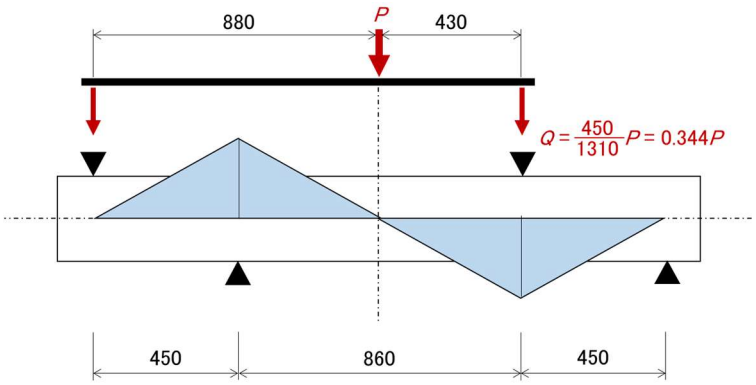

Fig. 3 Bending moment diagram

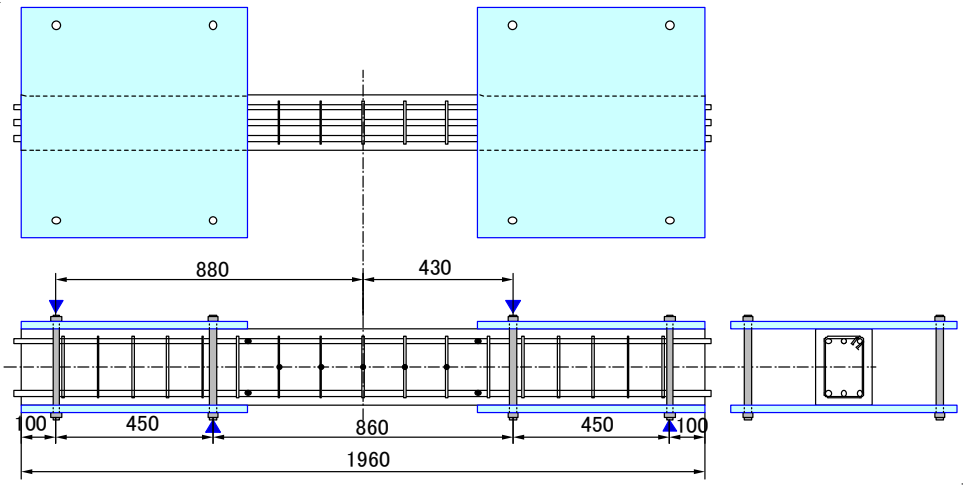

Fig. 4 Steel plate jackets for beam specimen

Fig. 5 State of loading

Two LVDTs were set to measure loading point displacements via holding jig fixing at the supporting points of the beam specimen as shown in Fig. 6. Assuming the rotation of rigid bodies of the specimen ends jacketed by the steel plates, translational angle (R) is obtained from relative displacement at the center of the specimen (δ) divided by clear span length. The strains of stirrups and longitudinal bars at the both ends of clear span were measured by strain gauges.

These loading and measurement method are consistent with those in previous study [6].

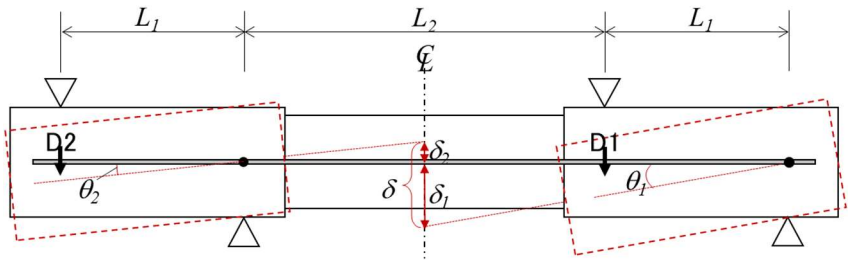

Fig. 6 Measurement method

3. Tensile characteristics of DFRCC by four-point bending test

3.1 Specimen and loading method

Table 4 shows the mixture proportion of DFRCC and compression test results by φ100mm x 200mm cylinder test pieces at the age of loading of beam specimens. Used cement was high-early-strength Portland cement, fly ash was Type II of Japanese Industrial Standard (JIS A 6202), and sand was size under 0.2mm. The high-range water-reducing admixture and thickening agent were added.

The specimen dimensions for four-point bending test are 100mm x 100mm in cross-section, and 400mm in length, these follows ISO 21914, "Test methods for fibre-reinforced cementitious composites – Bending moment - Curvature curve by four-point bending test" [7]. Axial deformation at upper and lower side in constant moment region were measured by pi-type LVDTs as shown in Fig. 7. Three specimens were tested for one-type of DFRCC.

Table 4 Mixture proportion of DFRCC

ID	Unit weight (kg/mm^3)					Comp. strength (MPa)	Elastic modulus (GPa)
	Water	Cement	Sand	Fly ash	Fiber		
NF-D4	380	678	484	291	-	47.2	16.3
NF-D6						43.0	15.1
PVA10-D4					13	45.3	16.8
PVA10-D6						49.1	16.6
PVA20-D4					26	43.1	15.7
PVA20-D6						50.6	15.7
PVA'05-D4					6.5	48.8	16.7
PVA'05-D6						51.9	17.1
AR05-D4					7.0	47.3	16.3
AR05-D6						48.1	16.6

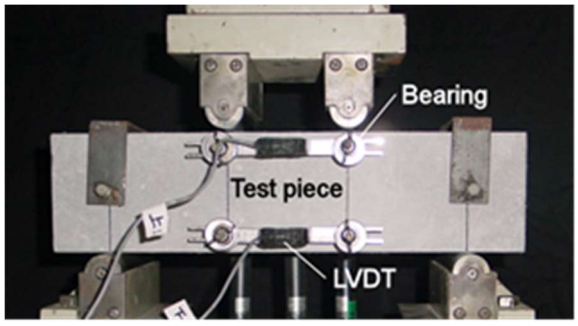

Fig. 7 Four-point bending test for DFRCC

3.2 Test results

Table 5 lists the test results of four-point bending test of DFRCC. Some specimens finally failed by opening of crack which took place outside of LVDT. Curvature at maximum load could not be obtained in these specimens. Most of the specimens showed deflection hardening behavior as that the load increased after first cracking.

Tensile strength and ultimate strain are calculated following ISO 21914 Annex A "Method of estimating tensile strength and average ultimate tensile strain" [7]. In this evaluation method, tensile strength can be calculated under the assumption that the tensile stress distributes as a constant manner in tension zone of the

section. Though this assumption is mostly accepted in the case of ECC, it is considered that the actual stress distribution in the case without strain hardening DFRCC is different from the assumed distribution.

The average values of tensile strength in each type of specimens are used for evaluation of shear capacity of beam specimen in Section 4.3. However, tensile strength of PVA'05-D4 specimens could not obtained because all of three specimens failed by crack outside LVDTs. Therefore, the same value as PVA'05-D6 is used for evaluation in PVA'05-D4 specimen.

Table 5 Test results of four-point bending test of DFRCC

ID	At maximum load		Calculation results		
	Curvature (1/m)	Bending moment (kN・m)	Ultimate strain (%)	Tensile strength (MPa)	Average tensile strength (MPa)
PVA10-D4	0.172	0.562	1.58	1.18	1.05
	0.093	0.528	0.82	1.16	
	0.066	0.413	0.66	0.82	
PVA10-D6	0.172	0.553	1.58	1.16	1.07
	0.106	0.481	0.96	1.02	
	0.091	0.485	0.81	1.03	
PVA20-D4	0.162	0.869	1.44	1.88	1.90
	0.088	0.866	0.74	1.93	
	—*1	0.737	—	—	
PVA20-D6	—*1	0.882	—	—	1.84
	0.259	0.872	2.37	1.83	
	0.280	0.882	2.57	1.84	
PVA'05-D4	—*1	0.590	—	—	(1.24)
	—*1	0.543	—	—	
	—*1	0.470	—	—	
PVA'05-D6	—*1	0.464	—	—	1.24
	0.004	0.402	0.02	1.32	
	0.006	0.404	0.04	1.15	
AR05-D4	0.114	0.419	1.04	0.91	1.31
	0.011	0.607	0.07	1.70	
	—*1	0.606	—	—	
AR05-D6	0.038	0.797	0.30	1.90	1.90
	0.048	—*2	0.44	—	
	0.035	—*2	0.32	—	

*1: Specimen failed by crack outside LVDTs.
*2: Measurement failure due to malfunction of testing machine

4. Test results of beam specimens and discussions

4.1 Failure progress

Beam specimens after loading are shown in Fig. 8. Cracks are traced by a pen after unloading. At first, small bending cracks took place at the ends of clear span in tension zone. After that, diagonal shear cracks were observed in the central part of the specimens. In NF specimens, the shear crack widely opened after yielding of stirrups, and shear force reached maximum value. Cover mortar fell from the specimens after maximum load.

In six specimens reinforced with PVA fibers (both φ100μ and φ27μ), small shear cracks took place in sequence. Except for PVA10-D4 and PVA'05-D6 specimens, shear force reached maximum value with

gradual localization of crack opening. On the other hand, in PVA10-D4 and PVA'05-D6 specimens, maximum load was observed at the same time of rapid localization of crack opening.

In AR specimens, multiple fine cracks took place in sequence, and maximum load was observed at the same time of rapid crack opening of some shear cracks. Until reaching maximum load, crack width was much smaller than the other specimens. Falling of covers were not observed in all fiber reinforced specimens. In all specimens, yielding of stirrups was observed before reaching the maximum load.

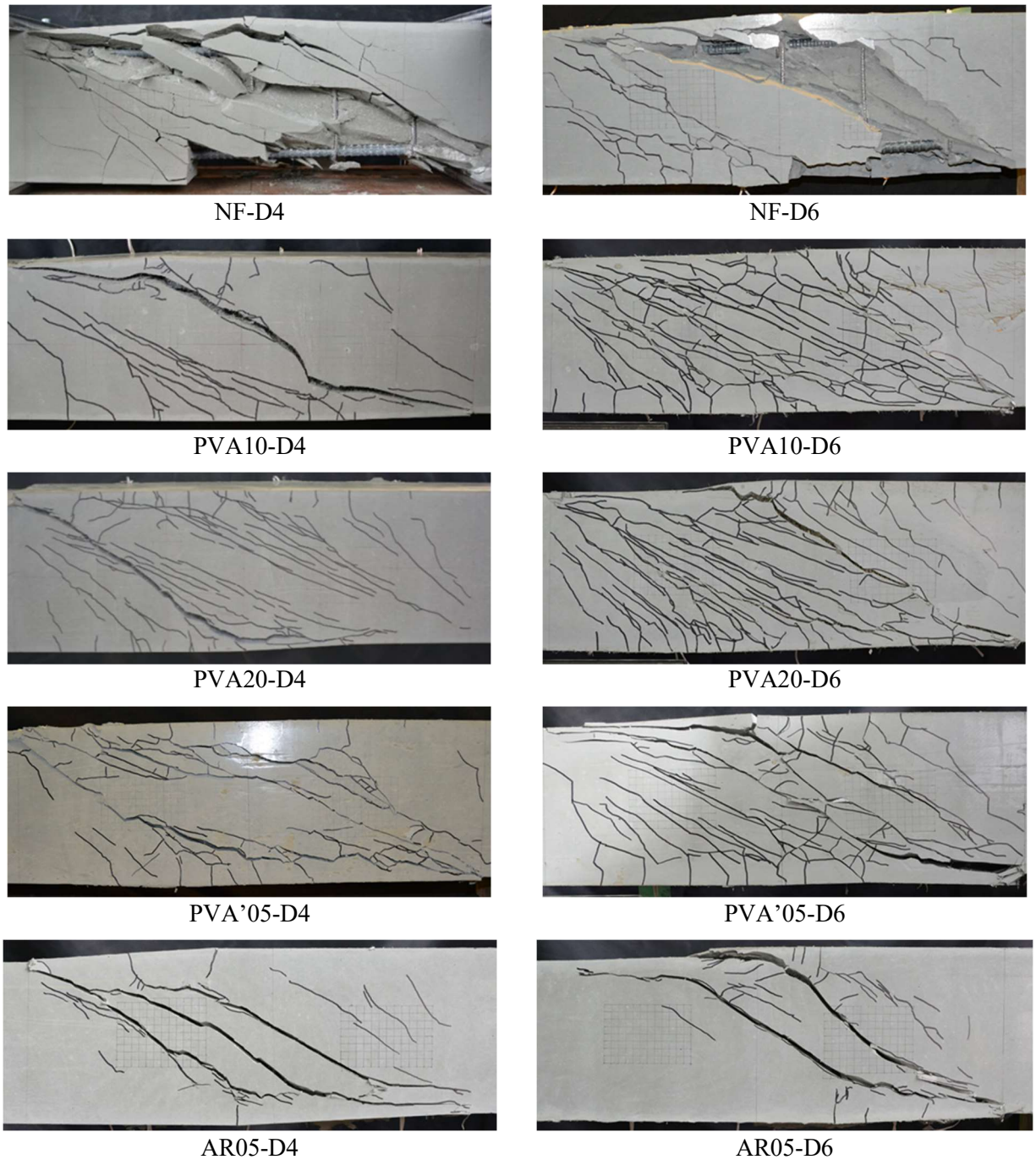

Fig. 8 Specimens after loading

4.2 Shear force-translational angle curve

Fig. 9 shows shear force (Q) - translational angle (R) curves of all specimens. Except for PVA10-D4 and PVA'05-D6 specimens, the maximum shear forces of the fiber reinforced specimens are larger than those of NF specimens with same type of stirrups. It is considered that shear force is carried also by fibers bridging at cracks.

On the other hand, in PVA10-D4 and PVA'05-D6 specimens, it is assumed that bridging effect of fibers vanished before reaching maximum load due to the rapid localization of shear crack as mentioned in Section 4.1. For this reason, it is considered that fibers could not increase the shear capacity in these specimens.

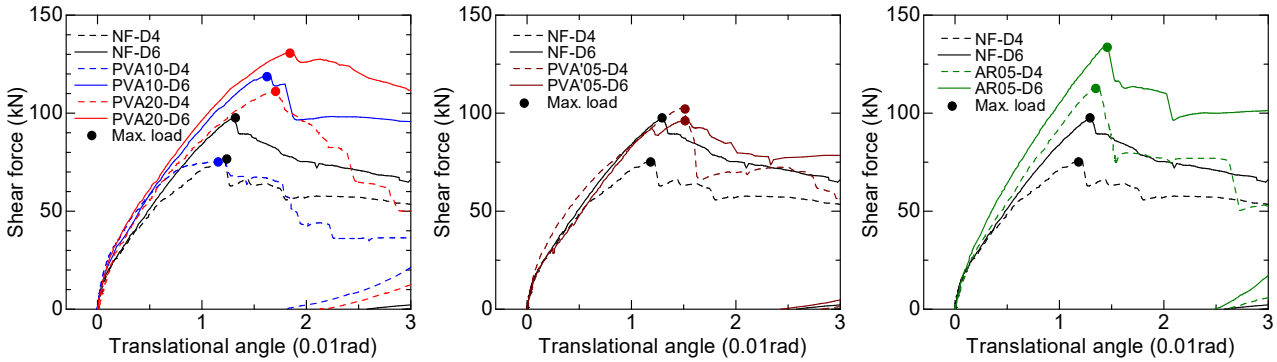

PVA (φ100μ) series PVA' (φ27μ) series AR series

Fig. 9 Shear force – translational angle curve

4.3 Evaluation of shear capacity of beam specimen

In the case of ECC, the evaluation method of shear capacity of beam has been propose by Eq.(1) [5]. This formula consists of shear capacity by truss (V_t) and arch (V_a) mechanism, and fiber bridging (V_f). Each shear capacity is given by Eq. (2) to Eq. (8). The former two items are same as the case of the conventional RC beams. Shear capacity by fiber bridging is simply added to consider the contribution of tensile stress of DFRCC. In this study, the same evaluation method is adopted for evaluation of shear capacity of DFRCC beams.

$$V_{su} = V_t + V_a + V_f \tag{1}$$

$$V_t = b \cdot j_t \cdot p_w \cdot \sigma_{wy} \cdot \cot\phi \tag{2}$$

$$V_a = \frac{\tan\theta \cdot (1-\beta) \cdot \nu \cdot \sigma_B \cdot b \cdot D}{2} \tag{3}$$

$$\tan\theta = \sqrt{\left(\frac{L}{D}\right)^2 + 1} - \left(\frac{L}{D}\right) \tag{4}$$

$$\beta = \frac{(1+\cot^2\phi) \cdot p_w \cdot \sigma_{wy}}{\nu \cdot \sigma_B} \tag{5}$$

$$\nu = 1.70{\sigma_B}^{-0.333} \tag{6}$$

$$\cot\phi = min\left\{2.0, \frac{j_t}{D \cdot \tan\theta}, \sqrt{\frac{\nu \cdot \sigma_B}{p_w \cdot \sigma_{wy}} - 1}\right\} \tag{7}$$

$$V_f = b \cdot j_t \cdot \nu_t \cdot \sigma_t \cdot \cot\phi \tag{8}$$

where,

V_{su} : shear capacity
V_t : shear capacity by truss mechanism
V_a : shear capacity by arch mechanism
V_f : shear capacity by fiber bridging
b : width of member
j_t : distance between compression and tension bars
p_w : stirrup ratio
σ_{wy} : yield strength of stirrup
σ_B : compression strength of DFRCC
ϕ : angle of compressive strut
θ : angle of arch mechanism
ν : effective coefficient of compressive strength of DFRCC
D : depth of member
L : clear span length
ν_t : reduction factor for tensile strength of DFRCC
σ_t : tensile strength of DFRCC

Table 6 lists the test results of shear capacity and calculation results by Eq.(1). The tensile strength of DFRCC listed in Table 5 is utilized for the calculation. Fig. 8 shows the comparison between the test results of shear capacity and calculation results. Both shear capacity is standardized by calculated flexural capacity of beam specimen considering fiber bridging in tension zone as indicated by Eq.(9) [8].

$$V_{fu} = 0.9\left\{a_t \cdot \sigma_y \cdot d + \frac{b \cdot D^2}{2}\sigma_t\right\}/(L/2) \tag{9}$$

where,

V_{fu} : flexural capacity
a_t : cross-sectional area of tension bars
σ_y : yield strength of tension bars
d : effective depth of member

As seen in Table 6 and Fig. 10, the calculated shear capacity overestimates the test results in PVA10-D4 and PVA'05-D6 specimens. In the loading test, these specimens show non-increasing of shear capacity by adding fibers. However, except for these two specimens, the ratios of test results to calculations exist from 0.90 to 1.05. It can be said that calculations show good agreements with the test results. Shear capacities of DFRCC beams can be evaluated by adding the effect of fiber-carrying capacity to calculated shear capacity in the case of no-fiber.

Table 6 Shear capacity of beam specimen

ID	Test result (kN)	Calculation (kN)	Test / Calc.
NF-D4	76.1	82.8	0.92
NF-D6	97.7	103.4	0.94
PVA10-D4	75.1	101.7	0.74
PVA10-D6	119.3	130.0	0.92
PVA20-D4	110.9	116.5	0.95
PVA20-D6	131.2	146.4	0.90
PVA'05-D4	102.8	108.1	0.95
PVA'05-D6	96.9	135.8	0.71
AR05-D4	113.7	108.1	1.05
AR05-D6	134.4	145.4	0.92

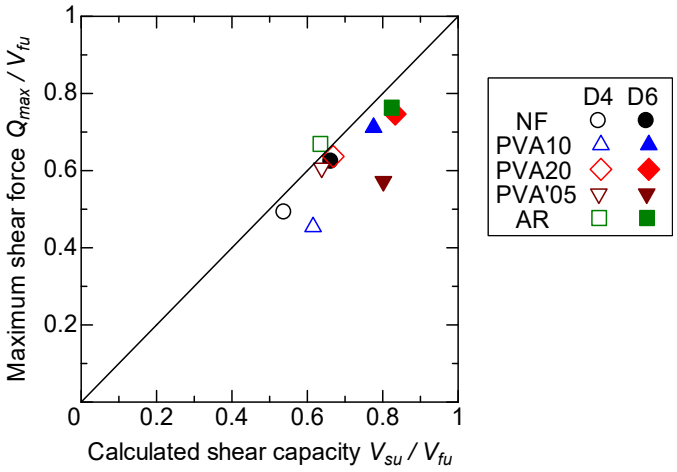

Fig. 10 Comparison of shear capacity

5. Conclusions

In this study, to evaluate shear behavior of seismic components using DFRCC with PVA and aramid fibers, beam specimens were subjected to anti-symmetrical bending moment loading. The test parameters are fiber types, volume fraction of fibers and diameter of stirrups. According to the test results, in most of the specimens with fibers, the shear capacities increased comparing to the mortar specimens. The fiber carrying capacity is calculated by using the tensile strength of DFRCC obtained from four-point bending test. The shear capacities are evaluated by adding the effect of fiber-carrying capacity to calculated shear capacity in the case of no-fiber. Calculated shear capacities of DFRCC show good agreements with the test results.

6. Acknowledgements

This study was supported by the JSPS KAKENHI Grant Number 18H03802.

7. References

[1] Li, V.C. (2019): Engineered Cementitious Composites (ECC): Bendable Concrete for Sustainable and Resilient Infrastructure, 1st ed., Springer

[2] Kanda, T., Tomoe, S., Nagai, S., Maruta, M., Kanakubo, T., Shimizu, K. (2006): Full Scale Processing Investigation for ECC Pre-cast Structural Element, *Journal of Asian Architecture and Building Engineering*, Vol.5, No.2, pp.333-340.

[3] Sano, N., Yamada, H., Miyaguchi, M., Yasojima, A., Kanakubo, T. (2015): Structural Performance of Beam-Column Joint using DFRCC, *11th Canadian Conference on Earthquake Engineering -Facing Seismic Risk-*, Paper ID 94163

[4] Rokugo, K., Kanda, T., ed. (2012): Strain Hardening Cement Composites: Structural Design and Performance, *State-of-the-Art Report of the RILEM Technical Committee 208-HFC*, RILEM State-of-the-Art Reports 6

[5] Kanakubo, T., Shimizu, K., Kanda, T., Nagai, S. (2007): Evaluation of Bending and Shear Capacities of HPFRCC Members toward the Structural Application, *Proceedings of the Hokkaido University COE Workshop on High Performance Fiber Reinforced Composites for Sustainable Infrastructure System*, pp.35-44.

[6] Kanakubo, T., Ozu, Y., Namiki, K., (2019): Shear behavior of DFRCC coupling beams using PVA and steel fiber, *Proceedings of The 2019 World Congress on Advances in Structural Engineering and Mechanics (ASEM19)*

[7] ISO 21914 (2019), Test method for fibre-reinforced cementitious composites – Bending moment - Curvature curve by four-point bending test.

[8] Shimizu, K., Kudo, S., Kanakubo, T. (2007), Scale Effect in Flexural and Shear Behavior on Ductile Reinforced Cementitious Composites, *Proceedings of the Japan Concrete Institute*, Vol. 29, No.3, 1429-1434. (in Japanese)

